

CIRCUMSTELLAR DUST DISKS AROUND STARS WITH KNOWN PLANETARY COMPANIONS

D. E. TRILLING,^{1,2} R. H. BROWN,^{1,3} AND A. S. RIVKIN¹

Lunar and Planetary Laboratory, University of Arizona, Tucson, AZ 85721

Received 1999 August 31; accepted 1999 September 7

ABSTRACT

We have searched six stars with known radial velocity planetary companions for circumstellar disks. Disks are expected around stars with planetary systems that accreted from regular protoplanetary disks, and remnant disks are expected to be similar to our solar system's Kuiper Belt. To date, we have detected circumstellar disks around three such stars: 55 Cnc, ρ CrB, and HD 210277. All these systems now resemble mature planetary systems with Jupiter-mass companions and Kuiper Belt-like disks. Our previous detection of the 55 Cnc disk (Trilling & Brown) is included here to place that disk in the context of the other two newly detected disks. Measuring the inclinations of the disks and assuming the disks are coplanar with the planets' orbits determines the masses of the planets around these three stars to be $1.9^{+1.1}_{-0.4} M_J$, $1.5^{+0.2}_{-0.1} M_J$, and $2.2^{+0.6}_{-0.2} M_J$, respectively ($1 M_J$ is one Jupiter mass). We also report nondetections for three stars—51 Peg, v And, and Gl876—that are known to have radial velocity companions. A number of possibilities exist to explain nondetections of disks, from the absence of a disk to limits on disk mass, radial extent, or inclination. We may also be looking through a disk's central hole, especially for the nearby star Gl876. The radial brightness profiles of each of the observed disks follow a power law with index ~ -5 , including a power of -2 from the stellar flux drop off, similar to the suggested value for our solar system's Kuiper Belt. This likely suggests that uniform physical processes govern the Kuiper Belt's population out to at least 100 AU, and may be ubiquitous among disks. Last, we discuss how disk characterizations can lead us toward refining theories of planetary system formation.

Subject headings: circumstellar matter — Kuiper Belt, Oort Cloud — planetary systems — solar system: formation

1. INTRODUCTION

We are conducting a survey of circumstellar disks around stars with known radial velocity companions. The reasons for this are twofold: first, we can directly image regions of planetary systems that are unseen in our solar system, and, by proxy, learn about the outer regions of our own solar system. Second, the detection of circumstellar disks around stars with known planetary companions strongly implies that the canonical disk-formation model is largely correct. We can also measure the inclinations of the detected disks, thus by implication removing the $\sin i$ ambiguity in the masses of the detected planets (Marcy et al. 2000). The null results we have found for three stars with known radial velocity companions indicate that some disks may be too small, too big, or have the wrong geometry to be detected; or alternately, that some systems with known radial velocity companions may not have related disks. This last point provides data to consider whether planets must form out of disks or not, or whether all observed companions are planets.

2. OBSERVATIONAL TECHNIQUE

Our observations were made at NASA's Infrared Telescope Facility (IRTF) on Mauna Kea, Hawaii, in 1998 February, June, and August. We used CoCo, the Cold

Coronagraph, which is a cryogenically cooled Lyot coronagraphic front end to NSFCAM (Wang et al. 1994; Toomey et al. 1998; Rayner et al. 1993; Shure et al. 1994). We also employed the new tip-tilt system (Smith & Onaka 1997) at the IRTF to improve centering of the stars behind the coronagraphic mask. CoCo has a Gaussian apodized focal plane mask with selectable and articulatable Lyot stops and acts as a two-dimensional Fourier filter, blocking light from the central star as well as light diffracted from the edges of the primary mirror and Cassegrain hole, allowing imaging to within 1.5 (27 pixels) of the center of the central star (Trilling & Brown 1998; Toomey et al. 1998). We routinely achieve a flux ratio of disk to unmasked central star of 10^{-5} , and a pixel-to-pixel noise of around 30 nJy at H band ($1.62 \mu\text{m}$), where most of our observations were made. ($1 \text{ Jansky} = 1 \text{ Jy} = 10^{-12} \text{ W m}^{-2} \mu\text{m}^{-1}$ at H band.) Since we observe in the near IR, we are most sensitive to light from the central stars reflected off of μm -sized dust particles. All stars are observed at less than 1.5 air masses. The seeing was typically around $0''.6$, though on occasion as good as $0''.4$. Only high-quality data in which a star is precisely centered behind the coronagraphic mask is used, so approximately 30% of data collected is discarded during data reduction. CoCo is very good at rejecting a large amount of the central star's light and also at preserving a smooth point-spread function (PSF) for the target stars (in other words, the coronagraph does not introduce any diffraction rings or spikes). It is because of the exceptional performance of CoCo that we are able to image these faint disks.

Our technique is to image several "PSF stars" of similar spectral type to our target star and not known to have any companions, and subtract the PSF of these comparison stars from that of the target star. The PSF stars are

¹ Visiting Astronomer at the Infrared Telescope Facility, which is operated by the University of Hawaii under contract to the National Aeronautics and Space Administration.

² Current address: UCO/Lick Observatory, University of California, Santa Cruz, CA 95064; trilling@ucolick.org.

³ Also at Steward Observatory, University of Arizona, Tucson, AZ 85721.

observed at the same air mass and very nearby on the sky to our target star (typically a few degrees away). The measured PSFs from these comparison stars are then subtracted from the target stars, to reveal any residual flux around the target star. For an ideal PSF subtraction, any residual flux after the PSF subtraction would represent flux from the target star system. In reality, observing conditions vary; because of this, we use three or more PSF comparison stars for every target star.

The target star's PSF (as convolved with the Gaussian coronagraphic mask) is assumed to be the same as that of the PSF star. Subtraction of each comparison star's stellar halo (PSF) from that of the target star is performed in turn, producing three different results for each set of target star observations. Reducing the data by comparing to several different PSF stars gives greater confidence in any findings and increases signal-to-noise for the residual flux. We have confidence in our detection of flux excess when it is reproduced around the target star for all three PSF different subtractions. It is important to emphasize that the PSF we use to subtract from the target star is not an analytic or model PSF, but rather a measured PSF. This allows us to reproduce (and subtract) the actual observed PSF from the target star, and accounts for any potentially varying observing conditions or changes in PSF with telescope altitude or temperature (focus). To determine the stability of the PSF during our observations and demonstrate the effectiveness of our technique, we intercompare our PSF stars, subtracting the PSF of one from that of the other. The results of this are shown in Figure 2 and described below. This differenced image is extremely flat; this demonstrates that the PSFs of the two stars are equivalent to a level of 10^{-7} times the peak flux from the central star or more.

In subtracting PSFs, we co-align the target and comparison stars to the nearest half-pixel; typically, the shift between the two is much less than a pixel. It is critical that all stars be directly centered behind the coronagraphic mask; much care was taken during our observing to ensure this, to the greatest possible precision. The IRTF's tip-tilt secondary aids us in retaining the star's position relative to the coronagraphic mask once it has been centered. Regardless, during data reduction, the centering of the star in each image is examined closely. Images in which the star has a centering asymmetry of greater than 1 pixel are typically discarded.

We demonstrate our technique—including PSF stability and co-centering accuracy—by comparing two PSF stars, producing a PSF-subtracted image that has no excess flux of the kind we have associated with circumstellar disks (see Fig. 2).

Flux calibration is carried out in the usual way, by observing standard flux stars from the Elias faint star list (Elias et al. 1982) at the same air masses and calibrating the on-chip flux with the known physical fluxes from the standards. Our peak surface brightness for the disks is typically around 1–5 mJy arcsec $^{-2}$, and the average post-reduction background cutoff is typically around 0.03–0.05 mJy arcsec $^{-2}$ (6–30 and 0.18–0.3 dNs, respectively). For all data presented here, the pixel-to-pixel 1σ noise is around 0.01 mJy arcsec $^{-2}$ (0.06 dNs).

3. RESULTS

We have observed six stars with known radial velocity companions. All the companions have minimum masses

around 1 Jupiter mass ($1 M_J$ is 1 Jupiter mass, 2×10^{30} g). We have detected circumstellar disks around three of the six stars. We previously reported the presence of a disk around 55 Cnc, a 3 billion year old star at a distance of 12.53 pc (Trilling & Brown 1998), consistent with the 60 μ m observations of Dominik et al. (1998), which imply the presence of a dusty disk. Figure 1 shows the H -band image of this disk. An ellipse describes the projection of a circular, inclined disk on the sky: a face-on disk (inclination of zero) will appear circular and an edge-on disk (inclination of 90°) will appear linear. If we assume that the disk we observe is circular and coplanar with the planet's orbit (which it should be if the planet and the disk both formed out of a regular protoplanetary environment and there was no post-formation processing that altered the plane of the planet's orbit), then by measuring the aspect ratio of the ellipse, we can determine the inclination of the disk on the sky, and therefore the inclination of the planet's orbit on the sky. Since the Doppler-shift radial-velocity technique determines the mass of a planet to within a factor of the sine of the inclination of the orbit of the planet, by solving for the inclination of the orbit, we find the mass of the planet. For 55 Cnc, the mass of the planet, in Jupiter masses, is $0.84 = M_p \sin i$ (Butler et al. 1997). We have found an inclination of 27_{-11}^{+8} degrees, giving a planetary mass of $1.9_{-0.4}^{+1.1} M_J$ (Trilling & Brown 1998). Peak surface brightness of the disk is around 3 mJy arcsec $^{-2}$; a small distance (~ 30 pixels, corresponding to the range 19–40 AU) along the radial axis has a value larger than 0.1 mJy arcsec $^{-2}$. The position angle is $50^\circ \pm 10^\circ$.

We have found a circumstellar dust disk around the star ρ CrB (Fig. 1). This star, a 10 billion year old G0 Sun-like star, was found to have a radial velocity companion whose semimajor axis is 0.23 AU and whose mass, in Jupiter masses, is $1.1 = M_p \sin i$ (Noyes et al. 1997). We have imaged this star on two separate occasions and found a disk whose major axis is oriented nearly north-south and which extends from the star to a distance of roughly 4", which corresponds to around 70 AU at the distance of ρ CrB, 17.53 pc (ESA 1997). Figure 1 shows the H -band image of this disk. We measure a disk inclination of 46_{-7}^{+4} degrees, which gives a planetary mass of $1.5_{-0.1}^{+0.2} M_J$. Peak surface brightness is around 1 mJy arcsec $^{-2}$, and surface brightness is larger than 0.1 mJy arcsec $^{-2}$ for 16 pixels radially (around 0.9", corresponding to the range 27–42 AU). The position angle is $5^\circ \pm 5^\circ$. The apparent asymmetry of the disk may be caused by a very low-level asymmetry in the PSF, by improper co-centering of the target and PSF stars, or by an actual asymmetry of the disk. Additional observations are necessary to determine the significance of the apparent observed asymmetry.

We have also detected a disk around the star HD 210277 (Fig. 1), with a peak surface brightness of 0.9 mJy arcsec $^{-2}$. The surface brightness is greater than 0.1 mJy arcsec $^{-2}$ for ~ 25 pixels, corresponding to the range 33–62 AU at the distance of HD 210277, 21.29 pc (ESA 1997). The position angle of the disk is $40^\circ \pm 10^\circ$. This image (Fig. 1) is a 2 minute exposure, demonstrating that this disk is bright and that when our technique works well and the seeing is exceptional, we can detect faint disks in a very short amount of time. We have around 30 minutes total integration time on this object, but this 2 minute exposure is the most dramatic and demonstrative. HD 210277 is a roughly 12 billion year old solar-type star (Marcy et al. 1999, Gon-

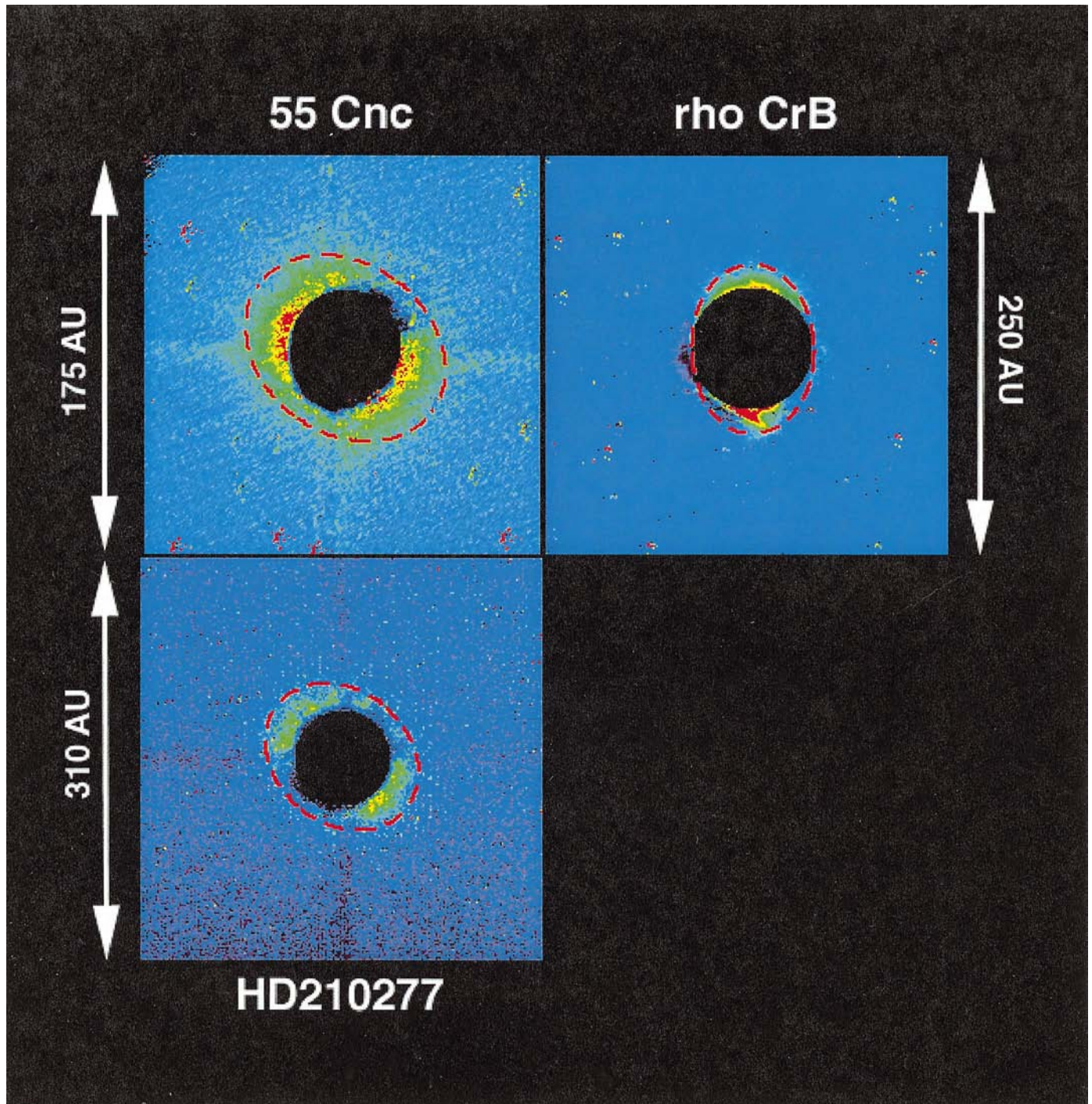


FIG. 1.—*H*-band images of the three circumstellar disks that we have detected to date. North is to the top and east is left. The black circle in the center of the images is the coronagraphic mask; we cannot image inside of this circle. The mask is around $3''$ in diameter. The red dashed line roughly represents an outer isophot of the disk (flux excess). The integration times are as follows: 55 Cnc, 58 minutes; ρ CrB, 50 minutes; HD 210277, 2 minutes. Special note should be made of the exceptional detection of the disk around HD 210277 in a 2 minute exposure. This 2 minute exposure is shown to emphasize our best result; we integrated, total, on HD 210277 for 32 minutes, but this image is less impressive than the 2 minute exposure shown here. All images have the same stretch and color table applied to them. The color table is linear, with the peak (*red*) corresponding to $1.81 \text{ mJy arcsec}^{-2}$, and the minimum (*blue*) corresponding to $0 \text{ mJy arcsec}^{-2}$.

zalez, Wallerstein, & Saar 1999). The radial velocity companion around this star has $M_p \sin i$ equal to $1.37 M_J$ (Marcy et al. 1999). If, as before, we assume that the disk is circular and coplanar with the planet's orbit, then we find an inclination of 39^{+5}_{-7} degrees and a companion mass of $2.2^{+0.6}_{-0.2} M_J$. However, HD 210277b, the planet, has an orbital eccentricity of 0.45. Since gas-disk formation tends to inhibit high eccentricities (Goldreich & Tremaine 1980),

it is likely that if the planet formed in a regular protoplanetary disk, the planet's eccentricity was increased in some postformation event. Many mechanisms that alter a planet's eccentricity also alter its inclination (for example, body-body interactions, as in Levison, Lissauer, Duncan 1998, Weidenschilling & Marzari 1996, Rasio & Ford 1996, and Holman, Touma, & Tremaine 1997). Therefore, the assumption that the planet is in the same plane as the disk is

questionable in this case: the planet may have been moved out of the formation plane. If the planet is not in the plane of the disk, then the mass of the companion remains unknown. Unfortunately, there currently is no way to determine whether the planet orbits in the same plane as the disk.

We did not detect a disk around the stars 51 Peg (G2.5 IV, 15.36 pc, 8.5 Ga), ν And (F8 V, 13.74 pc, 3 Ga), and G1876 (M5, 4.7 pc, 1–10 Ga) (Mayor & Queloz 1995; Marcy

et al. 1997; Butler et al. 1997; Marcy et al. 1998) (Fig. 2). The background surface brightness is around $0.05 \text{ mJy arcsec}^{-2}$ or less, so if there are disks there, the surface brightness of these disks must be less than that for us not to have detected them. 51 Peg and ν And are both solar-type stars, and appear as similar to our own sun as do the stars around which we have detected disks. In fact, there are no obvious differences among the solar-type stars we have observed: of

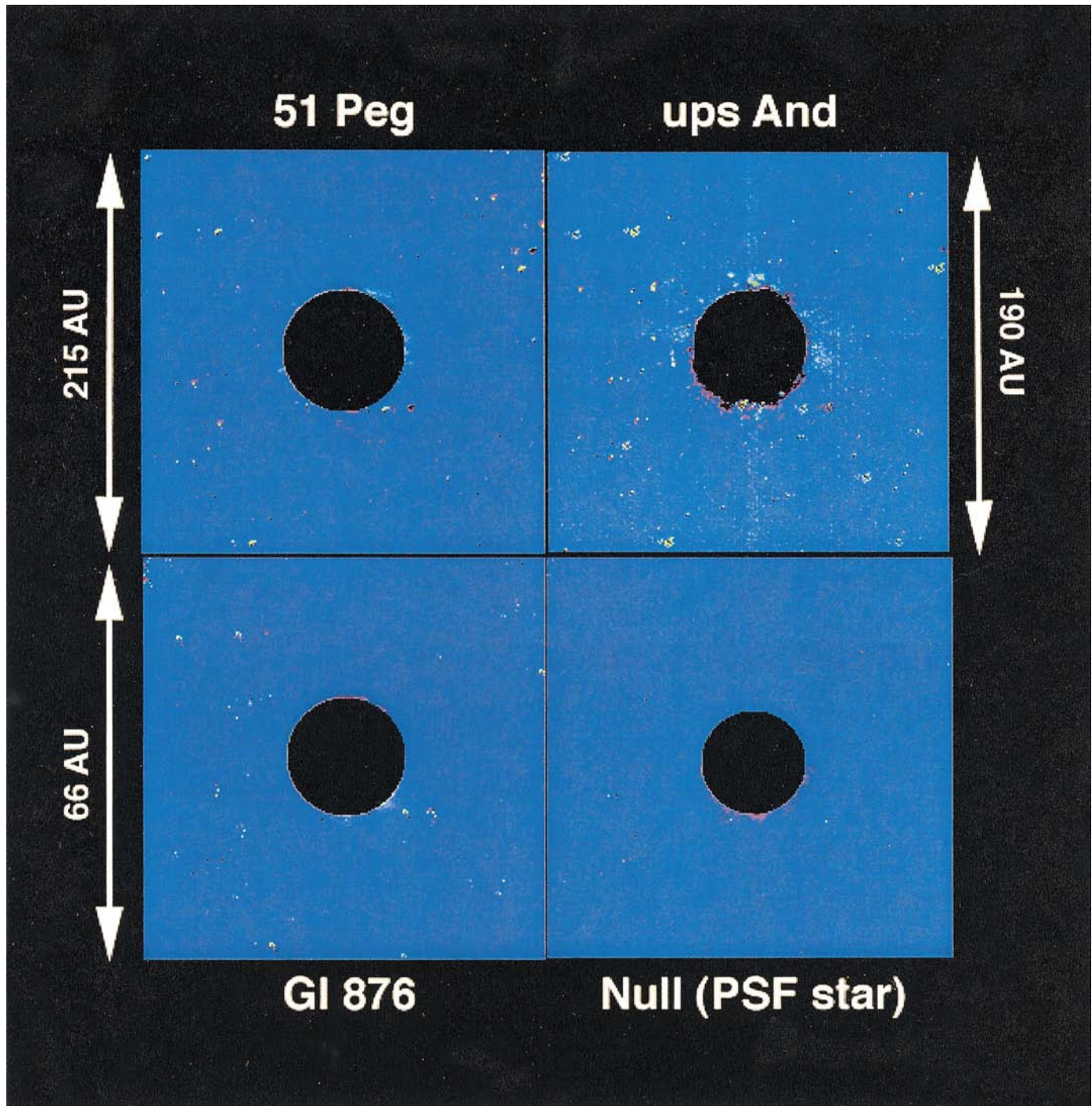


FIG. 2.—*H*-band images of three stars around which we did not detect circumstellar disks, plus two PSF stars; similar to Fig. 1. Each of these three stars (51 Peg, ν And, G1876) has a radial-velocity companion. The fourth frame is an intercomparison of two PSF stars, HD 210752 and HD 211080, both of which are G0 stars without known radial-velocity companions. The scaling and stretch on these images is the same as that on the images in Fig. 1. The integration times are as follows: 51 Peg, 24 minutes; ν And, 56 minutes; and G1876, 12 minutes. The integration time for the two PSF stars is 4 minutes. These two PSF star images were taken at nearly the same time as the 2 minute image of HD 210277 in Fig. 1. Exceptionally good seeing must have been present during this part of the night.

the five Sun-like stars we observed, three have detected disks and two do not.

4. DISCUSSION

Figure 3 shows radial profiles of the observed disks. We have azimuthally summed the fluxes of the disks about 50° centered on the major axes (in other words, $\pm 25^\circ$ from the disk's position angle) and plotted surface brightness against radial distance from the central star. Because the three detected disks are at different distances from the Earth, they cover a range of distances from the central star. The outer edge of the coronagraphic mask gives the innermost disk edge for the closest star (around 20 AU for the 55 Cnc disk), and the outermost disk edge (100+ AU for HD 210277) is given by the detection limit for that observation, the farthest star of the three. The peak surface brightness for all three disks is around 1–3 mJy arcsec $^{-2}$, and the surface brightness detection limit is around 30 μ Jy arcsec $^{-2}$, based on 3σ detections. Also shown is the radial profile of a null result, ν And.

We also show in Figure 3 models for disks massing 10^{-1} , 1, 10, 10^2 , 10^3 , and 10^4 times our Kuiper Belt's mass. (The mass of our Kuiper Belt [M_{KB}] is taken to be $4 \times 10^{-2} M_{\text{Earth}}$ (Weissman 1995, Duncan & Levison 1997).) These model disks are optically thin and are based on the assumption that the Kuiper Belt is a collisionally evolved

system with $N(d) \propto d^{-3.5}$, where N is the number of particles with diameter d (Farinella & Davis 1996; Dohnanyi 1969). We also assume that we observe light reflected off of greater than $1 \mu\text{m}$ sized Lambertian, spherical dust grains with albedo ~ 0.06 (Brown et al. 1997; Luu & Jewitt 1996; Jewitt, Luu, & Chen 1996). The masses of the model disks change inversely and linearly with the assumed albedo. The best-fit power-law index for the surface brightness change with radial distance in the detected disks is -5 ± 0.5 . This power-law index physically corresponds to a combination of an r^{-2} falloff from stellar flux and an r^{-3} falloff from the surface density of the disk. A constant power-law index over the range 25–100 AU implies that the surface density function is roughly constant over that range, as has been predicted (Duncan & Levison 1997). Duncan & Levison (1997) also find that our Kuiper Belt's surface density has a power-law index of about -3.5 . We find that a value of -3 is more appropriate, but in reasonable agreement; our error bars for the observed power-law index are about 0.5. There is relatively little change in the apparent optical depth of the disk with changing inclination of the disk until the disk is nearly edge-on. For inclinations greater than $\sim 75^\circ$, the radial profile function would include a convolution of a sine function with the power law, where the sine function represents the azimuth along the disk and would be seen as an additional radial function in a major axis profile. None of

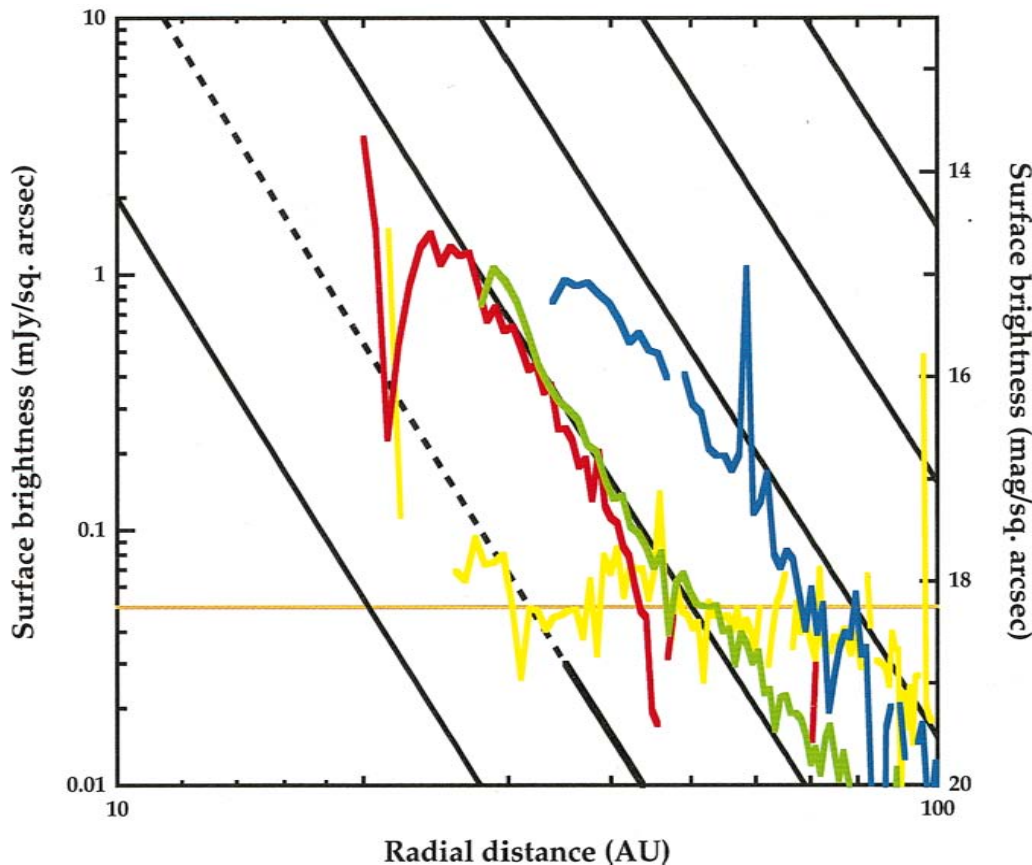


FIG. 3.—Radial profiles of circumstellar disks. Radial profiles of the three detected disks (55 Cnc, red; ρ CrB, green; and HD 210277, blue) and one null result (ν And, yellow) are shown, in mJy and magnitudes per square arcsecond, as a function of distance from the central star. Also shown is a conservative case background detection limit of $0.05 \text{ mJy arcsec}^{-2}$ (horizontal brown line). Model dust disks, with masses 0.1 , 1 , 10 , 100 , 1000 , and $10^4 M_{\text{KB}}$, are diagonal black lines, from lower left to upper right; our solar system's Kuiper Belt ($1 M_{\text{KB}}$) is the thick dot-dash line. The dotted part of the $1 M_{\text{KB}}$ line represents the inner hole of our Kuiper Belt; the solid part represents the part of the $1 M_{\text{KB}}$ model where dust would be found. This is near but below our current detection limit. The detected disks all have power-law indices around -5 ± 0.5 ; ν And shows a flat profile, indicative of a nondetection. The HD 210277 disk is detected to greater than 100 AU. (The right axis of the comparable plot in Trilling & Brown [1998] was mislabeled; the magnitudes shown in this figure are correct.)

our observed disks are close enough to edge-on for this additional factor to be significant.

The disks around 55 Cnc and ρ CrB are approximately 10 times more massive, and the HD 210277 disk is around 50–80 times more massive, than our Kuiper Belt. By comparison, the disk observed around β Pictoris is around 10^4 times as massive as our solar system's dust, and extends from around 50 AU out to at least 1000 AU (see, for example, Smith & Terrile 1984; Artymowicz 1997; Lagage & Pantin 1994). The observed disks are still relatively small compared to the mass of Jupiter; yet, a disk 50–80 times more massive than our Kuiper Belt would be a significantly more crowded place than our outer solar system.

The $1 M_{\text{KB}}$ profile in Figure 3 shows approximately what would be observed around our solar system (*dotted-solid line*). A worthwhile comment is that our solar system's Kuiper Belt has its inner edge around 35 AU. The $1 M_{\text{KB}}$ disk is above the detection limit for $a < 35$ AU (*dotted line*). Outside of 35 AU, our Kuiper Belt exists, but is below the detection limit (solid portion of the line). Therefore, as seen from another star, our solar system would almost but not quite be detectable because of background noise. However, if our Kuiper Belt had its inner edge closer to the Sun than 35 AU, as both 55 Cnc and ρ CrB do, then it would be detectable.

The largest radial extent of a disk we have observed is around 100 AU, for the HD 210277 disk. We know very little about this outer region of our solar system. As we show in Figure 3, a power-law slope of -5 reproduces the observed radial profiles from 25 AU out to around 100 AU. This suggests that the same processes—collisional evolution and grinding together of particles—govern the HD 210277 disk, at 100 AU, as govern our Kuiper Belt at 50 AU. Note that a constant power-law slope of -5 from 25 AU to more than 100 AU suggests that there does not seem to be a “depleted” region between an evolved inner population and a more primordial, outer region, as has been suggested (Stern & Colwell 1997); such a distribution would produce a change in the radial profiles presented in Figure 3. Since radiation pressure and Poynting-Robertson drag both would clear out μm -sized particles on short timescales, even at 100 AU, regeneration of dust particles by collisional grinding is required. The implication is that there are bodies grinding together and producing μm -sized dust out to at least 100 AU in normal-type solar systems' circumstellar disks.

Our Kuiper Belt models and discussion are not meant to provide a unique or complete model of either the Kuiper Belt or our observed disks. Instead, we simply point out the similarities between these observed disks and what is known about our own Kuiper Belt, similarities in mass, radial extent, and surface density profile. More rigorous models of these disks could certainly be created, and may be warranted at some point. Additionally, we hope in the near future to detect additional disks in this ongoing observing program, thus expanding the catalog and allowing more comparisons.

We detected no disk around three stars with known radial velocity companions: 51 Peg, ν And, and G1876. There are several possible interpretations of these nondetections:

1. These stars do not possess dust disks of the kind we have observed around 55 Cnc, ρ CrB, and HD 210277.

Since the kind of dust we observe is likely a requisite by-product of the grinding together of larger bodies, the lack of dust disk may be extended to the possibility of a lack of larger bodies as well. Although we believe that the formation of a remnant disk such as our Kuiper Belt is implicit in the formation of planets, these three null results may indicate that is not the case. If no Kuiper Belt-like disks exist around these three stars, either their planets formed by a different mechanism than did the planets around the Sun, 55 Cnc, ρ CrB, and HD 210277; or else the companions around these three stars are not planets, but rather stars, formed in co-collapse.

2. There is a disk there but we did not detect it because it is not massive enough. Figure 3 shows our current detection limit for disks, which is $\sim 0.1 M_{\text{KB}}$. This estimate assumes that the dust extends inward to at least 20 AU. A similar possibility to low disk mass is that the albedo is remarkably low, so there is less reflected light from the disk. If a disk were to have an inner edge at 35 AU, the minimum detectable disk mass would be much larger, around $3 M_{\text{KB}}$ or so (Fig. 3).

3. There is a disk there but we did not detect it because of the angular size of the disk. If the disk is smaller than the coronagraphic mask, or large enough that we are looking through an inner disk hole, then it would not be detected by us. Of particular note is the G1876 system. At 4.7 pc, this system is quite favorable for high spatial resolution imaging: the outer edge of the coronagraphic mask lies less than 10 AU from the central star. A notable possibility is that we could be looking through a hole in the disk, and that the disk could be entirely outside our field of view (about $5''$ radius, or 25 AU for G1876). Nondetection in the case of looking through the disk's hole corresponds to a minimum disk inner edge of 25 AU for an inclination of 0° (face-on); for an inclination of 45° , the inner edge of the disk must be at greater distance than about 35 AU. Both of these values are plausible for the inner edge of a disk; the inner edge of our Kuiper Belt is around 35 AU. For 51 Peg and ν And, the disks' inner edges would have to be around 40–50 AU or more, depending on the inclination of the system.

4. There is a disk there, but we did not detect it because of geometrical considerations—if all three systems had disks that were nearly face-on to the Earth. Our technique in theory works equally well for disks of any inclination; in practice, however, a disk with circular excesses around the coronagraphic mask might not be detected because circular isophots could be confused with a star's point-spread function, and not recognized as a reflected-light disk. In practice, a face-on disk ($i < \sim 20^\circ$) would produce a noisy signal around the coronagraphic mask, but not necessarily a coherently interpretable signal. However, although we would have a more difficult time detecting face-on disks, it might be expected that there would be fewer disks that are face-on, as follows: A face-on disk implies a low inclination ($i \rightarrow 0$). Low inclination means large companion mass, from $(\sin i)^{-1}$. A large companion mass indicates a star or brown dwarf, which do not require disk formation. So fewer disks at low inclinations might be expected.

In the interest of placing limits on nondetections, therefore, nondetections reveal either an angular extent less than $\sim 2''$; inner disk holes whose inner edges are in the 35–100

AU region, depending on the star; a disk mass less than around $0.1 M_{\text{KB}}$; or an inclination less than 20° . For combinations of these, the limits become less stringent. We note again that our own Kuiper Belt would be just below our current detection limit.

A last point of discussion is that Gl876 is an M star, unlike all the other stars we have observed, which are G or late F stars—near-solar analogs. Current thinking about planet formation typically focuses on G stars, for convenience and as the most interesting cases so far, by anthropocentric reasoning. It may be that some properties of M star formation and coeval planetary system formation inhibit disk or even planet formation, either because of luminosity differences or initial mass differences. Studying more M stars, both by radial velocity techniques and by our coronagraphic technique, will allow us to extend our ideas of planetary system formation to M stars in the interest of learning what relevant parameters govern the formation of planets.

That we have detected disks around three of the six stars with known radial velocity companions (it may be that one (or more) of our nondetection stars actually has a disk around it as well) implies a fairly high prevalence of disks around stars with planets, perhaps showing that remnant disk formation is indeed a part of planetary system formation, as has been suspected for our solar system. All these systems now resemble mature planetary systems with Jupiter-mass companions and Kuiper Belt–like disks. Con-

tinued study, through various techniques, will allow us to determine what are the relationships between disks and planets, and to what extent one necessarily implies the other. This in turn will allow us to revise and improve models of how planetary systems form. We will continue to study disks to look for correlations among disk mass, planet mass, planet heliocentric distance, and other observables, as well as to constrain the theory that giant planets migrate inward from their formation locations (Lin, Bodenheimer, & Richardson 1996; Trilling et al. 1998; Murray et al. 1998). We will also continue to study these six systems, to look deeper to extend the radial coverage for those stars with disks, and to search for the presence of fainter disks around those stars that so far show no circumstellar disks. Of particular interest will be continued, deeper studies of the ν And system, in light of the recent announcement of the presence of two additional planets in that system (Butler et al. 1999).

The authors greatly appreciate advice, suggestions, and sharing of target lists from Geoff Marcy in advance of publication. Doug Toomey, Christ Ftaclas, and Norm Murray provided useful assistance at the telescope, with data reduction, and discussion of results, respectively. We thank the IRTF for supporting for this project. This work is supported by NASA grants to D. E. T. and R. H. B.

REFERENCES

- Artymowicz, P. 1997, *Ann. Rev. Earth Planet. Sci.*, 25, 175
 Brown, R. H., Cruikshank, D. P., Pendleton, Y., & Veeder, G. J. 1997, *Science*, 276, 937
 Butler, R. P., Marcy, G. W., Williams, E., Hauser, H., & Shirts, P. 1997, *ApJ*, 474, L115
 Butler, R. P., et al. 1999, *ApJ*, 526, 916
 Dohnanyi, J. S. 1969, *J. Geophys. Res.*, 74, 2531
 Dominik, C., Laureijs, R. J., Jourdan de Muizon, M., & Habing, H. J. 1998, *A&A*, 329, L53
 Duncan, M. J., & Levison, H. F. 1997, *Science*, 276, 1670
 Elias, J. H., Frogel, J. A., Matthews, K., & Neugebauer, G. 1982, *AJ*, 87, 1029
 ESA. 1997, *The Hipparcos and Tycho Catalogues* (ESA SP-1200; Noordwijk: ESA)
 Farinella, P., & Davis, D. R. 1996, *Science*, 273, 938
 Goldreich, P., & Tremaine, S. 1980, *ApJ*, 241, 425
 Gonzalez, G., Wallerstein, G., & Saar, S. H. 1999, *ApJ*, 511, L111
 Holman, M., Touma, J., & Tremaine, S. 1997, *Nature*, 386, 254
 Jewitt, D. C., Luu, J. X., & Chen, J. 1996, *AJ*, 112, 1225
 Lagage, P. O., & Pantin, E. 1994, *Nature*, 369, 628
 Levison, H. F., Lissauer, J. J., & Duncan, M. J. 1998, *AJ*, 116, 1998
 Lin, D. N. C., Bodenheimer, P., & Richardson, D. C. 1996, *Nature*, 380, 606
 Luu, J. X., & Jewitt, D. C. 1996, *AJ*, 111, 499
 Marcy, G. W., Butler, R. P., Vogt, S. S., Fischer, D., & Lissauer, J. J. 1998, *ApJ*, 505, L147
 Marcy, G. W., Butler, R. P., Vogt, S. S., Fischer, D., & Liu, M. 1999, *ApJ*, 520, 239
 Marcy, G. W., Butler, R. P., Williams, E., Bildsten, L., Graham, J. R., Ghez, A. M., & Jernigan, J. G. 1997, *ApJ*, 481, 926
 Marcy, G. W., Cochran, W. D., & Mayor, M. 2000, in *Protostars and Protoplanets IV*, ed. V. Mannings et al. (Tucson: Univ. Arizona Press), in press
 Mayor, M., & Queloz, D. 1995, *Nature*, 378, 355
 Murray, N., Hansen, B., Holman, M., & Tremaine, S. 1998, *Science*, 279, 69
 Noyes, R. W., Jha, S., Korzennik, S. G., Brown, T. M., Kennelly, E. J., & Horner, S. D. 1997, *ApJ*, 483, L111
 Rasio, F. A., & Ford, E. B. 1996, *Science*, 274, 954
 Rayner, J. T., et al. 1993, *Proc. SPIE*, 1946, 490
 Shure, M., et al. 1994, *Exp. Astron.*, 3, 239
 Smith, S. S., & Onaka, P. M. 1997, *Proc. SPIE*, 3112, 275
 Smith, B. A., & Terrile, R. J. 1984, *Science*, 226, 1421
 Stern, S. A., & Colwell, J. E. 1997, *ApJ*, 490, 879
 Toomey, D. W., Ftaclas, C., Brown, R. H., & Trilling, D. 1998, *Proc. SPIE*, 3354, 782
 Trilling, D. E., Benz, W., Guillot, T., Lunine, J. I., Hubbard, W. B., & Burrows, A. 1998, *ApJ*, 500, 428
 Trilling, D. E., & Brown, R. H. 1998, *Nature*, 395, 775
 Wang, S.-I., et al. 1994, *Proc. SPIE*, 2198, 578
 Weidenschilling, S. J., & Marzari, F. 1996, *Nature*, 384, 619
 Weissman, P. 1995, *ARA&A*, 33, 327